Observations on variational and projector Monte Carlo methods

C. J. Umrigar

Citation: The Journal of Chemical Physics **143**, 164105 (2015); doi: 10.1063/1.4933112
View online: https://doi.org/10.1063/1.4933112
View Table of Contents: http://aip.scitation.org/toc/jcp/143/16
Published by the American Institute of Physics

Observations on variational and projector Monte Carlo methods

C. J. Umrigar[a)]
Laboratory of Atomic and Solid State Physics, Cornell University, Ithaca, New York 14853, USA

(Received 1 June 2015; accepted 21 September 2015; published online 26 October 2015)

Variational Monte Carlo and various projector Monte Carlo (PMC) methods are presented in a unified manner. Similarities and differences between the methods and choices made in designing the methods are discussed. Both methods where the Monte Carlo walk is performed in a discrete space and methods where it is performed in a continuous space are considered. It is pointed out that the usual prescription for importance sampling may not be advantageous depending on the particular quantum Monte Carlo method used and the observables of interest, so alternate prescriptions are presented. The nature of the sign problem is discussed for various versions of PMC methods. A prescription for an exact PMC method in real space, i.e., a method that does not make a fixed-node or similar approximation and does not have a finite basis error, is presented. This method is likely to be practical for systems with a small number of electrons. Approximate PMC methods that are applicable to larger systems and go beyond the fixed-node approximation are also discussed. © *2015 AIP Publishing LLC.* [http://dx.doi.org/10.1063/1.4933112]

I. INTRODUCTION

Quantum Monte Carlo (QMC) methods[1–7] are accurate and versatile methods for treating quantum many-body systems. The two most commonly used classes of QMC methods used for pure-state systems are the variational Monte Carlo (VMC) method and various projector Monte Carlo (PMC) methods.

PMC methods are stochastic implementations of the power method for determining expectation values of operators for the dominant eigenstate (the one with the largest absolute eigenvalue) of a matrix or integral kernel. They are useful when the Hilbert space is so large (typically $>10^{10}$ states) that it is impractical to store a single vector of the size of the Hilbert space, leave alone a matrix. In fact, they can be used even for infinite continuous Hilbert spaces and for a space that has both continuous and discrete degrees of freedom, e.g., space and spin or isospin. In the interest of brevity, we will use notation appropriate for discrete spaces (sums, matrices, etc.) interchangeably with notation appropriate for continuous spaces (integrals, integral kernels, etc.). If it is feasible to store a vector, then deterministic iterative diagonalization methods, such as the Lanczos method, are usually preferable since they do not have a statistical error. PMC methods get around the memory restriction by storing at any instant in time only a random sample of the vector elements and computing expectation values as a time average. The members of these samples are referred to as *walkers*.

In the context of QMC methods, a method is said to be *exact* if it has a statistical error (which goes down as the inverse square root of the computer time provided that the conditions for the central limit theorem are satisfied), but no systematic bias. PMC methods suffer from a *sign problem* except in some special situations. Consequently, they frequently employ an approximation, e.g., the *fixed-node* (FN) approximation[8,9] or in the case of complex wavefunctions, the *fixed-phase* approximation.[10] Although PMC methods do not require good trial wavefunctions, the systematic bias from such approximations is much reduced when optimized trial wavefunctions are used. Expectation values have no bias in the limit that the trial wavefunction is exact, and further, expectation values of operators that commute with the Hamiltonian have no statistical error either in this limit.

The VMC method is used to find expectation values of operators for a given trial wavefunction and to optimize[11–17] the parameters in the trial wavefunction. Since the accuracy and efficiency of approximate PMC methods also depend crucially on the trial wavefunction, it is normal procedure to first use VMC to optimize the trial wavefunction prior to doing the PMC calculation.

The outline of this paper is as follows. In Sec. II, the notation is introduced and the VMC method and various PMC methods are presented in a unified way. In Sec. III, the way that the sign problem manifests itself in the various methods is discussed and the pros and cons of various choices that are made in designing the algorithms are discussed. In Sec. IV, a continuous real-space algorithm is proposed for calculating the exact energy for small fermionic systems. In Sec. V, approximate algorithms that go beyond the fixed-node approximation and are applicable to larger systems are discussed. The Appendix has a discussion of optimal importance sampling and near optimal functions that can be efficient in practice. It also presents an efficient method for sampling the product of the fixed-node wavefunction and a nodeless guiding function, which can useful for reducing the statistical error of various expectation values.

II. FORMALISM

Consider a basis $\{\phi_i\}$ which may be complete or incomplete and continuous or discrete. Three functions are of interest, the exact wavefunction $|\Psi_0\rangle$, the trial wavefunction, $|\Psi_T\rangle$,

a)CyrusUmrigar@cornell.edu

and the guiding function, $|\Psi_G\rangle$. (If the basis is incomplete then "exact" will be used to mean "exact in that basis.") Each of these functions can be expanded in this basis,

$$\text{exact wavefunction:} \quad |\Psi_0\rangle = \sum_i e_i|\phi_i\rangle, \;\; e_i = \langle\phi_i|\Psi_0\rangle\,, \quad (1)$$

$$\text{trial wavefunction:} \quad |\Psi_T\rangle = \sum_i t_i|\phi_i\rangle, \;\; t_i = \langle\phi_i|\Psi_T\rangle\,, \quad (2)$$

$$\text{guiding function:} \quad |\Psi_G\rangle = \sum_i g_i|\phi_i\rangle, \;\; g_i = \langle\phi_i|\Psi_G\rangle\,. \quad (3)$$

The trial wavefunction, $|\Psi_T\rangle$, and the guiding function, $|\Psi_G\rangle$, are usually chosen to be the same function, but they play different roles and in many circumstances, large gains can be achieved by choosing them to be different. Ψ_T is used to calculate variational and mixed estimators of operators $\hat{A}$, i.e., $\langle\Psi_T|\hat{A}|\Psi_T\rangle/\langle\Psi_T|\Psi_T\rangle$ and $\langle\Psi_T|\hat{A}|\Psi_0\rangle/\langle\Psi_T|\Psi_0\rangle$. As such, the requirements on $|\Psi_T\rangle$ are that $A(i) = \frac{\langle\phi_i|\hat{A}|\Psi_T\rangle}{\langle\phi_i|\Psi_T\rangle}$ can be computed quickly, typically in time of $O(N^3)$ or better, where N is the number of particles, and that the local energy $E_L(i) = \frac{\langle\phi_i|\hat{H}|\Psi_T\rangle}{\langle\phi_i|\Psi_T\rangle}$ fluctuates as little as possible.

Ψ_G instead is used to choose the probability density that is sampled, i.e., Ψ_G^2 in VMC and $\Psi_G\Psi_0$ or $\Psi_G\Psi_{FN}$ in PMC. Consequently, Ψ_G must be such that $g_i \neq 0$ if $e_i \neq 0$. If Ψ_T also satisfies this condition, then Ψ_G can be chosen to be Ψ_T. Reasons to have $\Psi_G \neq \Psi_T$ are (a) to allow Ψ_T to be sparse, which may be necessary to enable rapid evaluation of the local energy, and (b) to reduce the variance of estimators of expectation values, in particular to have finite-variance rather than infinite-variance estimators for certain expectation values.

A. Variational Monte Carlo

The variational energy is

$$\begin{aligned}
E_V &= \frac{\langle\Psi_T|\hat{H}|\Psi_T\rangle}{\langle\Psi_T|\Psi_T\rangle} = \frac{\sum_{ij}^{N_{st}}\langle\Psi_T|\phi_i\rangle\langle\phi_i|\hat{H}|\phi_j\rangle\langle\phi_j|\Psi_T\rangle}{\sum_i^{N_{st}}\langle\Psi_T|\phi_i\rangle\langle\phi_i|\Psi_T\rangle} \\
&= \frac{\sum_{ij}^{N_{st}} t_i H_{ij} t_j}{\sum_i^{N_{st}} t_i^2} = \frac{\sum_i^{N_{st}} g_i^2 \frac{t_i^2}{g_i^2}\frac{\sum_j^{N_{st}} H_{ij}t_j}{t_i}}{\sum_i^{N_{st}} g_i^2 \frac{t_i^2}{g_i^2}} \\
&= \frac{\sum_i^{N_{st}} g_i^2 \frac{t_i^2}{g_i^2} E_L(i)}{\sum_i^{N_{st}} g_i^2 \frac{t_i^2}{g_i^2}} \\
&= \frac{\left[\sum_i^{N_{MC}} \frac{t_i^2}{g_i^2} E_L(i)\right]_{\Psi_G^2}}{\left[\sum_i^{N_{MC}} \frac{t_i^2}{g_i^2}\right]_{\Psi_G^2}} \equiv \frac{\left\langle \frac{t_i^2}{g_i^2} E_L(i)\right\rangle_{\Psi_G^2}}{\left\langle \frac{t_i^2}{g_i^2}\right\rangle_{\Psi_G^2}},
\end{aligned} \quad (4)$$

where N_{st} is the number of states (possibly infinite) in the Hilbert space and the local energy, $E_L(i)$, at state i is defined as

$$E_L(i) = \frac{\langle\phi_i|\hat{H}|\Psi_T\rangle}{\langle\phi_i|\Psi_T\rangle} = \frac{\sum_j^{N_{st}} H_{ij}t_j}{t_i}. \quad (5)$$

The notation in the last line of Eq. (4) indicates that the N_{MC} Monte Carlo points are sampled from the distribution Ψ_G^2 (usually using the Metropolis-Hastings algorithm[18,19]). The value of E_V depends only on Ψ_T, but the statistical error depends on Ψ_T and Ψ_G. Since $E_L(i) \to E_0$ in the limit that $\Psi_T \to \Psi_0$, the bias and statistical error of the energy estimator vanish as $\Psi_T \to \Psi_0$. For fixed Ψ_T, the usual choice, $\Psi_G = \Psi_T$, eliminates the fluctuations in the denominator but does not minimize the fluctuations of the energy. In fact for some expectation values of interest, e.g., the derivative of the energy with respect to a variational parameter, the choice $\Psi_G = \Psi_T$ yields an infinite-variance estimator, whereas a more intelligent choice for Ψ_G yields a finite-variance estimator. Various choices for Ψ_G are discussed in the Appendix. The choice $\Psi_G = \Psi_T$ does have the advantage that the quantum mechanical expectation value, E_V, becomes a single MC expectation value, rather than a ratio of MC expectation values. Since ratios of expectation values are not expectation values of ratios, the choice $\Psi_G = \Psi_T$ results in simpler expressions for unbiased quantum mechanical expectation values.

B. Projector Monte Carlo

Projector Monte Carlo methods, in common with the coupled cluster method, take advantage of the fact that the exact energy can be written as the mixed expectation value,

$$\begin{aligned}
E_0 &= \frac{\langle\Psi_0|\hat{H}|\Psi_T\rangle}{\langle\Psi_0|\Psi_T\rangle} = \frac{\sum_{ij}^{N_{st}}\langle\Psi_0|\phi_i\rangle\langle\phi_i|\hat{H}|\phi_j\rangle\langle\phi_j|\Psi_T\rangle}{\sum_i^{N_{st}}\langle\Psi_0|\phi_i\rangle\langle\phi_i|\Psi_T\rangle} \\
&= \frac{\sum_{ij}^{N_{st}} e_i H_{ij} t_j}{\sum_i^{N_{st}} e_i t_i} = \frac{\sum_i^{N_{st}} e_i g_i \frac{t_i}{g_i}\frac{\sum_j^{N_{st}} H_{ij}t_j}{t_i}}{\sum_i^{N_{st}} e_i g_i \frac{t_i}{g_i}} \\
&= \frac{\sum_i^{N_{st}} e_i g_i \frac{t_i}{g_i} E_L(i)}{\sum_i^{N_{st}} e_i g_i \frac{t_i}{g_i}} \\
&= \frac{\left[\sum_i^{N_{MC}} \frac{t_i}{g_i} E_L(i)\right]_{\Psi_G\Psi_0}}{\left[\sum_i^{N_{MC}} \frac{t_i}{g_i}\right]_{\Psi_G\Psi_0}} \equiv \frac{\left\langle \frac{t_i}{g_i} E_L(i)\right\rangle_{\Psi_G\Psi_0}}{\left\langle \frac{t_i}{g_i}\right\rangle_{\Psi_G\Psi_0}}.
\end{aligned} \quad (6)$$

If no approximations are made, the PMC energy is exact (it has no bias), independent of Ψ_T and Ψ_G, but the statistical error depends on Ψ_T and Ψ_G. In FN-PMC, Ψ_G is usually chosen to be Ψ_T and the statistical error depends on Ψ_T. In a discrete space, the bias depends on Ψ_T whereas in a continuous space, it depends only on the nodes of Ψ_T. As in the case of VMC, the statistical error and bias of the energy vanish as $\Psi_T \to \Psi_0$, since $E_L(i) = E_0$, independent of i.

1. Projectors

In VMC, the quantities appearing in the expectation values are explicitly known and so the distribution we choose to sample is also known and can be sampled using the Metropolis-Hastings algorithm.[18,19] In PMC, the quantities appearing in the expectation values involve the exact wavefunction, Ψ_0, or the fixed-node wavefunction, Ψ_{FN}, which are unknown. However, they can be sampled by repeated application of a *projector*. A projector, $\hat{P}(\tau)$, is any function of the Hamiltonian that has one eigenvalue equal to one, and all other eigenvalues of absolute magnitude smaller than one. Examples of projectors are the exponential projector, $\hat{P}(\tau) = e^{\tau(E_T\hat{1}-\hat{H})}$, also

known as the imaginary-time propagator, the linear projector, $\hat{\mathbf{1}} + \tau(E_T\hat{\mathbf{1}} - \hat{H})$, and $\frac{1}{\hat{\mathbf{1}}-\tau(E_T\hat{\mathbf{1}}-\hat{H})}$. I use the word "projector" rather loosely, since a large number of applications of $\hat{P}(\tau)$ onto an arbitrary state are required to project it onto the ground state $|\Psi_0\rangle$. Although there is no upper limit to τ for the exponential projector, in practice, rather small values of τ are used because known explicit expressions for it in the chosen basis become exact only in the $\tau \to 0$ limit. For the linear projector, there is a strict upper limit, $\tau < (E_{\max} - E_{\min})/2$; else, the dominant state of $\hat{P}$ is the highest state of $\hat{H}$ rather than the desired ground state of $\hat{H}$. Hence, it can be used only for Hamiltonians with bounded spectra.

2. Taxonomy of PMC methods

There exist several PMC methods that differ in many details, but they can be classified according to three important characteristics.

1. The form of the projector, $\hat{P}(\tau)$. The most common choices are the exponential projector, also known as the imaginary-time propagator, $\hat{P}(\tau) = \exp(\tau(E_T - \hat{H}))$, and the linear projector, $1 + \tau(E_T - \hat{H})$.
2. The choice of basis states, i.e., the space in which the MC walk is performed. Two examples are (a) real space, i.e., the states are specified by the positions of the N particles or (b) orbital occupation space, i.e., the states are specified by which orbitals are occupied.
3. Whether permutation symmetry is applied to the states or not, i.e., whether states that are related by permutation symmetry are considered to be the same state or different states. We will refer to unsymmetrized basis states as 1st-quantized states and symmetrized basis states as 2nd-quantized states.

Table I describes some commonly used PMC methods. For example, the diffusion Monte Carlo (DMC) method[8,20–23] uses $\hat{P} = e^{\tau(E_T\hat{\mathbf{1}}-\hat{H})}$ and 1st-quantized walkers in the space of electron coordinates, whereas the full configuration interaction quantum Monte Carlo (FCIQMC) method[24,25] and its semistochastic extension, the S-FCIQMC method[26] use $\hat{P} = \hat{\mathbf{1}} + \tau(E_T\hat{\mathbf{1}} - \hat{H})$ and 2nd-quantized walkers in the occupation number space of orthogonal orbitals.

3. Importance sampled projectors

The projector provides the way to sample the exact ground state wavefunction, Ψ_0, with components e_i. In MC methods, when calculating expectation values, we can always factor the integrand into a probability distribution and the remaining factor, which is the quantity that is averaged during the MC run. A good choice for the probability distribution can significantly reduce the statistical error of the MC estimate; this process is called *importance sampling*.

In the context of PMC, importance sampling is done by similarity transforming the projector,[27] with a diagonal matrix whose diagonal components are the components of the guiding function, Ψ_G. So, the importance-sampled projector $\tilde{P}$ has components,

$$\tilde{P}_{ij} = \frac{g_i P_{ij}}{g_j}. \tag{7}$$

Now, since

$$\sum_j P_{ij} e_j = e_i, \tag{8}$$

it can readily be verified that $\tilde{P}$ has a dominant eigenstate with eigenvalue 1 and elements $g_i e_i$,

$$\sum_j \tilde{P}_{ij}(g_j e_j) = \sum_j \left(\frac{g_i P_{ij}}{g_j}\right)(g_j e_j) = g_i e_i. \tag{9}$$

Hence, repeated application of $\tilde{P}$ results in sampling $\rho = \Psi_G\Psi_0$.

The efficiency of the algorithm depends not only on the projector but also on how it is sampled. For any given projector, it is always possible to sample it by first sampling from an arbitrary probability density and then reweighting the sampled point by the ratio of the projector to the sampled probability density at that point. Small weight fluctuations make for higher efficiency. In the ideal case, the probability density is proportional to the projector so that the reweighting factor becomes $\sum_i \tilde{P}_{ij}$ which is independent of the sampled point, i. This is called "heat-bath sampling."

Note that in the limit that $\Psi_G \to \Psi_0$,

$$\sum_i \tilde{P}_{ij} = 1, \tag{10}$$

so $\tilde{P}_{ij}$ becomes a *column-stochastic* matrix. Hence, in this limit if heat-bath sampling is used, the weights do not fluctuate at all.

Since QMC methods usually suffer from a sign problem, most QMC calculations make an approximation, e.g., the fixed-node approximation[8,9] in DMC and the phaseless approximation[30] in AFQMC. In the fixed-node approximation, the projection is done subject to the constraint that the projected state has the same nodes as Ψ_T. It is common practice in FN calculations to choose $\Psi_G = \Psi_T$. In calculations that go

TABLE I. Classification of some commonly used PMC methods by the form of the projector, the basis used, and its quantization. The annotation, "samp. τ," indicates that the value of τ is not fixed but is sampled from a probability density.

Method	Projector	1-particle basis	Quantization
DMC	$e^{\tau(E_T\hat{\mathbf{1}}-\hat{H})}$	$\mathbf{r}$	1st
GFMC (Refs. 27 and 28)	$e^{\tau(E_T\hat{\mathbf{1}}-\hat{H})}$ (samp. τ)	$\mathbf{r}$	1st
LRDMC (Ref. 29)	$\hat{\mathbf{1}}+\tau(E_T\hat{\mathbf{1}}-\hat{H})$	$\mathbf{r}_i$	1st
S-FCIQMC	$\hat{\mathbf{1}}+\tau(E_T\hat{\mathbf{1}}-\hat{H})$	ϕ_i^{orthog}	2nd
Phaseless AFQMC (Ref. 30)	$e^{\tau(E_T\hat{\mathbf{1}}-\hat{H})}$	$\phi_i^{\text{nonorthog}}$	2nd

beyond the fixed-node approximation, e.g., release-node calculations,[21,31,32] wherein the fixed-node constraint is released for a certain number of MC generations, it is common practice to use a nodeless Ψ_G (see, e.g., Eq. (23)) that approximates $|\Psi_T|$ far from the nodes of Ψ_T and is rounded off near the nodes of Ψ_T. However, this linkage — using $\Psi_G = \Psi_T$ for FN calculations and using a nodeless Ψ_G for methods that go beyond the FN approximation — is not required. In Section IV, we propose an exact DMC method that can use either a nodeless Ψ_G, or $\Psi_G = \Psi_T$. In the Appendix, we show that it is possible to do FN calculations by fixing the nodes with Ψ_T but using a nodeless Ψ_G for importance sampling. This has the benefit of reducing the statistical error of some expectation values; in particular, the variance of some estimators is altered from being infinite to being finite.

4. Growth estimator for the energy

The energy expression in Eq. (6) is called the "mixed energy" estimator since it is obtained from the mixed expectation value of $\hat{H}$ between $\langle\Psi_0|$ and $|\Psi_T\rangle$. Since $\hat{P}$ is a function of $\hat{H}$, the energy can also be obtained from computing a mixed expectation value of $\hat{P}$ between $\langle\Psi_0|$ and $|\Psi_G\rangle$, and then deducing the lowest eigenvalue of $\hat{H}$ from the largest eigenvalue of $\hat{P}$. This is the "growth" estimator. Of course, both of these estimators give the exact energy if no approximations such as the fixed-node approximation are made. If $\Psi_G = \Psi_T$, then not only are the expectation values of E_{mix} and E_{gr} close, but even the finite sample errors of E_{mix} and E_{gr} are close, since their difference comes only from the nonlinearity of $\hat{P}$ as a function of $\hat{H}$. Hence, e.g., in DMC, where it is normal practice to use $\Psi_G = \Psi_T$, E_{mix} and E_{gr} have nearly the same statistical error and $E_{mix} - E_{gr}$ is much smaller than either statistical error provided that no unnecessary weight fluctuations are introduced, i.e., provided that the split-join algorithm[23] or the stochastic reconfiguration algorithm,[33,34] rather than the integerization algorithm, is used to control the spread of walker weights. On the other hand, in the S-FCIQMC methods, $\Psi_G = \mathbf{1}$ is used and the growth and mixed estimators can have very different statistical errors.

C. Practicality of QMC methods

In order for VMC and PMC to be practical for reasonably large systems, it is essential that the cost of each of the following steps:

1. proposing the MC move,
2. computing g_i and t_i,
3. computing $E_L(i)$,

scale as a low-order polynomial in N. In the case of discrete-space QMC methods, the last requirement is satisfied usually by choosing a basis in which the Hamiltonian is sparse. In addition, Ψ_T is also sometimes chosen to be sparse. In the case of continuous real-space QMC methods, it is automatically satisfied since the potential energy is usually local in that basis unless nonlocal pseudopotentials are used, and the kinetic energy is obtained by taking the Laplacian of the trial wavefunction. In addition, in most cases, only approximate PMC calculations are practical because of the sign problem.

III. SIGN PROBLEM

PMC methods can suffer from a sign problem. Except for a few special situations, e.g., 1-dimensional problems in real space, fermionic systems almost always have a sign problem. In all PMC methods, the sign problem occurs because an undesired state grows relative to the state of interest when the system is evolved by repeated stochastic applications of the projector. This results in a computational cost that grows exponentially with system size N. A reasonable definition[3] is that there is no sign problem if the computer time required to compute the value of an observable for an N-particle system with specified error, ϵ, scales as $T \propto N^{\delta}\epsilon^{-2}$, where δ is a small power (say, $\delta \leq 4$). (It is assumed that N is increased in some approximately homogeneous way, e.g., adding more atoms of the same species.) The details of how the sign problem manifests itself is different in the various PMC methods, and we discuss two examples before making some more general comments on the sign problem.

A. Sign problem in DMC

DMC employs the exponential projector, $\hat{P}(\tau) = e^{\tau(E_T\hat{\mathbf{1}} - \hat{H})}$. The walk is done in the 1st-quantized space of electron coordinates, i.e., walkers are specified by the $3N$ coordinates of the N electrons and walkers that are related by a permutation of electron coordinates are considered as residing on different states.

An approximate projector in the real-space basis, usually referred to as a Green function in the context of DMC, is

$$G(\mathbf{R}', \mathbf{R}, \tau) \equiv \langle \mathbf{R}'|\hat{P}(\tau)|\mathbf{R}\rangle \approx \frac{e^{\frac{-(\mathbf{R}'-\mathbf{R})^2}{2\tau} + \left(E_T - \frac{\mathcal{V}(\mathbf{R}')+\mathcal{V}(\mathbf{R})}{2}\right)\tau}}{(2\pi\tau)^{3N/2}}. \quad (11)$$

It is nonnegative everywhere, so there is no sign problem if one were interested in the dominant state of this projector. However, the dominant state of this projector is the bosonic ground state whereas the state of interest is the fermionic ground state. If one started with a positive distribution and a negative distribution such that their sum is purely fermionic as illustrated in Fig. 1, and applied the projector deterministically, both the positive and the negative distributions would tend to the bosonic ground state, but their sum would yield the fermionic ground state, though with an amplitude that gets exponentially small relative to the amplitude of the individual components with increasing MC time. However, the projection is done stochastically and the probability of positive and negative walkers landing on the same state at the same MC time step and cancelling is very small if the portion of the state space that contributes significantly to the expectation values is finite and large, and it is zero if the state space is continuous (unless the dynamics of the walkers is modified to force opposite-sign walkers to land on the same spot). Hence, it is not possible to sum the positive and negative contributions

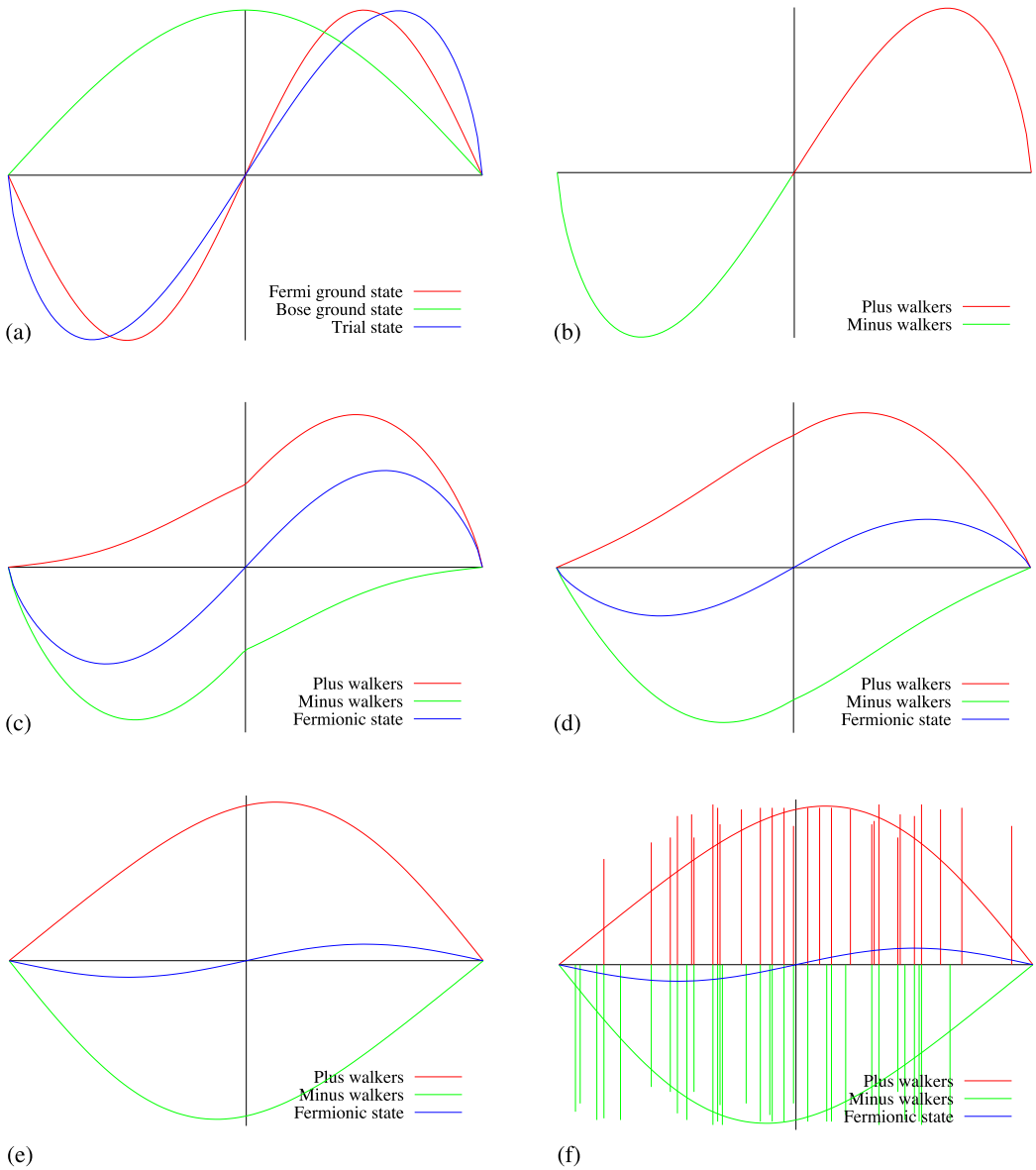

FIG. 1. Demonstration of the sign problem in DMC. (a) The green curve schematically depicts the bosonic ground state, the red curve the fermionic ground state, and the blue curve an approximate fermionic wavefunction. (b) The starting positive distribution is shown in red and the starting negative distribution in green. Their sum is purely fermionic. (c)-(f) The red and the green curves show the evolution of the positive and negative distributions. Their sum, the blue curve, converges to the fermionic ground state. (f) For a finite population, the walkers are depicted as delta functions and in a continuous space, they never meet and cancel (unless they are forced to in some way). Consequently, there is an exponentially vanishing "signal to noise" ratio.

to extract the fermionic ground state. This is demonstrated in Fig. 1. Furthermore, note that the problem cannot be solved by using an extremely large population of walkers. This enhances the probability of cancellations, but, because of fluctuations, eventually only positive or only negative walkers will survive and so the fermionic state will completely disappear.

B. Sign problem in S-FCIQMC

It may appear from the above discussion that the sign problem can be solved by performing the MC walk in a 2^{nd}-quantized, i.e., antisymmetrized, basis. Each 2nd-quantized basis state consists of all the permutations of the corresponding 1st-quantized basis states. Then, there are no bosonic states or states of any symmetry other than fermionic, so there is no possibility of getting noise from non-fermionic states. Of course, it is well known that this does not solve the sign problem. The problem is that different paths leading from a state to another can contribute with opposite sign. If the opposite sign contributions occur at the same MC step, then the contributions cancel and yield a net contribution of smaller absolute magnitude, just as they would in a deterministic calculation. The problem occurs when opposite sign contributions occur at different MC steps. Further, since Ψ and $-\Psi$ are equally good, they are each sampled with equal probability in the course of a long MC run.

In a few special situations, the sign problem is absent. The necessary and sufficient condition for there to be no sign problem is that all columns (or equivalently rows) of the projector have the same sign structure aside from an overall sign. Equivalently, there is no sign problem if it is possible to find a set of sign changes of the basis functions such that all elements

of the projector are nonnegative. For example, the projector with the following sign structure:

$$\begin{bmatrix} + & - & + & + \\ - & + & - & - \\ + & - & + & + \\ + & - & + & + \end{bmatrix} \tag{12}$$

does not have a sign problem, since changing the sign of the 2nd basis state makes all the elements nonnegative. Note that it is not necessary to actually make these sign changes — the projectors before and after the sign changes are equally good.

Although a 2nd-quantized basis does not solve the sign problem, it is advantageous to use a 2nd-quantized basis when designing an exact fermionic algorithm. First, an antisymmetrized basis is a factor of $N!$ smaller, and so, the probability of opposite sign walkers meeting and cancelling is greater. Second, since each 2nd-quantized basis state consists of a linear combination of 1st-quantized basis states, 2nd-quantized states that are connected by the projector may have multiple connections for each of the constituent 1st-quantized states. Hence, there is the possibility of internal cancellations in the 2nd-quantized basis, which reduces the severity of the sign problem.[35] Third, since bosonic and other symmetry states are eliminated, it is clear that one can achieve a stable signal to noise for any large but finite basis by making the walker population very large. The limit of an infinite walker population is equivalent to doing a deterministic projection, which of course does not have a sign problem.

Booth, Thom, and Alavi[24] did just this by inventing highly efficient algorithms for dealing with a large number of walkers and demonstrated that a finite signal to noise ratio and therefore accurate energies can be attained in practice for small molecules in a small basis, using a large but manageable number of walkers. The MC walk, in their FCIQMC method is done in an orbital occupation number (or equivalently determinantal) basis. In a subsequent paper, Cleland, Booth, and Alavi[25] introduced the *initiator approximation* which greatly reduces the walker population needed to achieve a stable signal to noise ratio. Only states that have more walkers on them than some threshold value can spawn walkers on states that are not already occupied. The associated initiator error disappears of course in the limit of an infinite population. However, it can be of either sign and it can be nonmonotonic, so extrapolation to the infinite population limit can be tricky. In subsequent papers, Alavi and coworkers have improved the efficiency of these calculations[36] and published calculations on various molecules, the homogeneous electron gas[37] at small r_s, and even solids,[37,38] though in a small basis. The related model space QMC (MSQMC) method[39] permits the calculation of quasi-degenerate excited states. In a recent paper,[40] the FCIQMC method has been extended to calculate the reduced 2-body density matrix, which allows for a variational estimate of the energy and therefore an easier extrapolation to the infinite population limit.

In many problems of interest, much of the spectral weight of the ground state is concentrated on a relatively small portion of the entire Hilbert space. Nevertheless, the rest of Hilbert space needs to be included in order to get sufficiently accurate results. The S-FCIQMC method[26] takes advantage of this. (This method was previously referred to as the semistochastic quantum Monte Carlo (SQMC) method.[26] In this paper, we call it S-FCIQMC to emphasize that it is an extension of the FCIQMC method.) The most important states are identified by an iterative procedure using 2nd-order perturbation theory. Transitions between these important states are done deterministically, whereas the rest of the transitions are done stochastically. Since deterministic projection has no sign problem and no statistical error, the severity of the sign problem and the magnitude of the statistical error are reduced. The S-FCIQMC method in fact makes two other important modifications to the FCIQMC method that result in greatly improved efficiency. First, Ψ_T is chosen to be an optimized linear combination of basis states (determinants), as opposed to just the Hartree-Fock state in the original FCIQMC method, and second, the S-FCIQMC method uses real weights for the walkers, whereas the original FCIQMC method used integer weights. The deterministic part of the projector and the local energy components (the numerators and the denominators of E_L) for all the connections to Ψ_T are precomputed and stored before the MC run since these elements are used at every MC step. These modifications result in efficiency gains of three orders of magnitude[26] using a deterministic space and Ψ_T of around 10^4 determinants on a single core. Since both the deterministic space matrix elements and the connections to Ψ_T can be distributed, much larger deterministic spaces and Ψ_T can be used on large parallel computers.

C. Discussion of sign problem

The nature of the sign problem in the FCIQMC method has been elucidated in Refs. 35 and 41. We briefly review some of the points made there and add a few more general observations since the nature of the sign problem depends on the three characteristics we used in the taxonomy of PMC methods.

Since the projector and the Hamiltonian are functions of each other, they share the same eigenstates and statements relating the dominant state and the dominant fermionic state of the projector can be turned into equivalent statements relating the ground state and the fermionic ground state of the Hamiltonian.

A 1st-quantized basis allows states of various symmetries and the sign problem occurs because the fermionic ground state of the Hamiltonian is not the dominant state of the projector. In real space, the projector has nonnegative off-diagonal elements, provided the potential is local. So the dominant state is entirely of one sign and is therefore the physical bosonic ground state of the Hamiltonian. The severity of the sign problem is related to the gap between the fermionic and bosonic ground states. In a discrete basis, one can reduce the severity of the sign problem by imposing the condition that no more than one electron can occupy any single particle state since then the relevant gap is smaller — it is between the fermionic and the hard-core bosonic ground states.

A 2nd-quantized basis allows only states of the correct symmetry. Unlike the 1st-quantized case, even in real space and using a local potential, the projector typically has some negative off-diagonal elements that cannot be eliminated by altering the sign of some of the states. The severity of the sign problem can be characterized by the gap between the dominant

state of the projector and the dominant state of the projector with all off-diagonal elements replaced by their absolute values[41] which need not be the physical bosonic state. This gap is always smaller than or equal to the relevant gap in the 1st-quantized basis.[35] If the gap is zero, then there is no sign problem. This has already been discussed in the case of FCIQMC in Ref. 41 but is generally true for 2nd-quantized bases.

MC methods that use an orbital basis, e.g. S-FCIQMC and AFQMC, have a less severe sign problem than methods that use a real space basis, e.g. DMC, in the following sense. For an independent particle Hamiltonian, e.g. Hartree-Fock, if the MC walk is performed in the space of determinants of the eigenorbitals of that Hamiltonian, then there is no sign problem since the projector is diagonal. The sign problem arises only from the difference of the true Hamiltonian from the independent particle Hamiltonian. Similarly, in the AFQMC method,[30] the independent particle part of the projector is treated deterministically and therefore has no sign problem. The severity of the sign problem depends on the choice of the orbitals and experience indicates that natural orbitals are often better than Hartree-Fock orbitals. In contrast, the DMC method has a sign problem even for independent particle Hamiltonians.

If a linear projector is used, there is little or no internal cancellation when using a 2nd-quantized basis. For example, there are no internal cancellations for the Hubbard model both in real space and in momentum space.[35] There is also no cancellation[35] for the *ab initio* Coulombic Hamiltonian in real space in the LRDMC method.[29] In contrast, the exponential projector has considerable internal cancellation for this Hamiltonian since all $N!$ permutations contribute to the weight of the final state, the even permutations with one sign and the odd permutations with the opposite sign. Even though there are $N!$ cancelling contributions, at small τ there will be little cancellation because the contribution from the identity permutation will dominate. So, it is important to have a projector with a small time step error so that a sufficiently large τ can be used. In addition to internal cancellation, one needs to have also inter-walker cancellation. This is more effective if the walkers are concentrated on a small number of states, so in this respect orbital space is preferable to real space. The AFQMC method[30] has both these desirable properties (exponential projector and 2nd-quantized orbital basis), but an effective cancellation scheme has yet to be devised. However, even in the absence of cancellations, accurate calculations for the Hubbard model and for the Cr_2 molecule in a finite basis have been done[42,43] using "free projection."

IV. EXACT PMC IN REAL SPACE

An important advantage of real-space PMC methods (e.g., DMC) compared to orbital-space PMC methods (S-FCIQMC and CP-AFQMC) is that an infinite continuous basis is used from the outset and so an extrapolation to infinite basis size is not required. In the S-FCIQMC approach, the computational cost to achieve a given statistical error goes up at least as $N_{\rm bas}^2$, where $N_{\rm bas}$ is the size of the single-particle basis if the MC moves are proposed from an approximately uniform distribution. Even if the MC moves are proposed using an approximate heat-bath algorithm,[44,45] i.e., the probabilities are roughly proportional to the projector matrix elements, the cost still goes up with basis size, but much more slowly. Hence, motivated by the success of the S-FCIQMC approach, it is reasonable to ask whether an exact PMC algorithm (i.e., one that does not make a fixed-node approximation) can be devised in real space. At first sight, it seems much harder to do this since in a continuous space walkers never land on the same state by accident and therefore never cancel. However, one can devise a dynamics that forces two or more walkers to move to the same state. Kalos and coworkers[46–52] and Anderson and coworkers[53,54] have for many years explored such approaches with only limited success. Accurate potential energy surfaces for 3- and 4-electron molecules have been computed.[53,54] The new ideas presented in this paper will hopefully lead to more widely useful algorithms.

The first thing to note is that it is advantageous to work in a 2nd-quantized rather than a 1st-quantized basis, but hitherto, this has not been done in real space. Each 2nd-quantized walker consists of $N!$ 1st-quantized walkers, i.e., there are 1st-quantized walkers at every permutation of $\mathbf{R} \equiv \mathbf{r}_1, \mathbf{r}_2, \ldots, \mathbf{r}_N$. When importance sampling is not used the walkers represent Ψ_0 so those at even permutations have one weight and those at odd permutations have minus that weight. When importance sampling is used, the walkers represent $\Psi_G\Psi_0$ and if Ψ_G is an antisymmetric function (e.g., Ψ_T), all permutations have the same weight. In either cases all permutations of course contribute equally to expectation values since the contributions contain a factor of Ψ_T/Ψ_G which cancels any possible sign change in the weights.

Starting from Eq. (11), the projector for the 2nd-quantized walkers could be obtained by summing the probabilities of all permutations of initial electron positions to evolve to final electron positions. This results in a determinantal form for the projector

$$G_2(\mathbf{R}', \mathbf{R}, \tau) = \begin{vmatrix} g(\mathbf{r}'_1, \mathbf{r}_1) & g(\mathbf{r}'_1, \mathbf{r}_2) & \cdots & g(\mathbf{r}'_1, \mathbf{r}_N) \\ g(\mathbf{r}'_2, \mathbf{r}_1) & g(\mathbf{r}'_2, \mathbf{r}_2) & \cdots & g(\mathbf{r}'_2, \mathbf{r}_N) \\ \vdots & & & \\ g(\mathbf{r}'_N, \mathbf{r}_1) & g(\mathbf{r}'_N, \mathbf{r}_2) & \cdots & g(\mathbf{r}'_N, \mathbf{r}_N) \end{vmatrix} \times e^{\left(E_T - \frac{\mathcal{V}(\mathbf{R}') + \mathcal{V}(\mathbf{R})}{2}\right)\tau}, \tag{13}$$

where

$$g(\mathbf{r}'_i, \mathbf{r}_j) = \frac{1}{\sqrt{2\pi\tau}} e^{\frac{-(\mathbf{r}'_i - \mathbf{r}'_j)^2}{2\tau}} \tag{14}$$

and $\mathcal{V}(\mathbf{R})$ is the potential energy. Note that the diagonal term from the expansion of the determinant is just the usual DMC projector in the absence of importance sampling shown in Eq. (11).

Of course, it is not practical to use this form of the projector since the potential energy $\mathcal{V}(\mathbf{R})$ diverges to $\pm\infty$ at particle coincidences. One can greatly improve upon this projector by using an antisymmetrized version of the pair-product projector used in path-integral Monte Carlo.[55] The pair-product projector contains both electron-nuclear and electron-electron

factors. The former, being single-particle in nature, can be antisymmetrized using a determinant. So, an approximate antisymmetric projector is

$$G_2(\mathbf{R}',\mathbf{R},\tau) = \begin{vmatrix} g(\mathbf{r}'_1,\mathbf{r}_1) & g(\mathbf{r}'_1,\mathbf{r}_2) & \cdots & g(\mathbf{r}'_1,\mathbf{r}_N) \\ g(\mathbf{r}'_2,\mathbf{r}_1) & g(\mathbf{r}'_2,\mathbf{r}_2) & \cdots & g(\mathbf{r}'_2,\mathbf{r}_N) \\ \vdots & & & \\ g(\mathbf{r}'_N,\mathbf{r}_1) & g(\mathbf{r}'_N,\mathbf{r}_2) & \cdots & g(\mathbf{r}'_N,\mathbf{r}_N) \end{vmatrix} \times e^{(E_T - U_{ee}(\mathbf{R}',\mathbf{R}))\tau}, \quad (15)$$

where $g(\mathbf{r}'_j,\mathbf{r}_i)$ is now the product of the pair projector of an electron moving from $\mathbf{r}_i$ to $\mathbf{r}'_j$ interacting with all the nuclei,

$$g(\mathbf{r}'_j,\mathbf{r}_i) = \prod_{\alpha=1}^{N_{nuc}} p_{en}(\mathbf{r}'_j - \mathbf{r}_\alpha, \mathbf{r}_i - \mathbf{r}_\alpha, \tau) \quad (16)$$

and $U_{ee}(\mathbf{R}',\mathbf{R})$ is either the end-point pair product action[55] of the electrons interacting with each other,

$$U_{ee}(\mathbf{R}',\mathbf{R}) = \sum_{i<j} \frac{u(\mathbf{r}'_{ij},\mathbf{r}'_{ij},\tau) + u(\mathbf{r}_{ij},\mathbf{r}_{ij},\tau)}{2}, \quad (17)$$

or the pair product action[55] of the electrons interacting with each other for the identity permutation,

$$U_{ee}(\mathbf{R}',\mathbf{R}) = \sum_{i<j} u(\mathbf{r}'_{ij},\mathbf{r}_{ij},\tau). \quad (18)$$

It is likely that antisymmetrizing the full pair-product projector would yield a more accurate projector, but the $O(N!)$ computational cost would be prohibitive, whereas the projector of Eq. (15) has only $O(N^3)$ cost.

The importance-sampled projector, $\tilde{G}_2(\mathbf{R}',\mathbf{R},\tau)$ is related to $G_2(\mathbf{R}',\mathbf{R},\tau)$ in the usual way,

$$\tilde{G}_2(\mathbf{R}',\mathbf{R},\tau) = \Psi_G(\mathbf{R}') G_2(\mathbf{R}',\mathbf{R},\tau) \frac{1}{\Psi_G(\mathbf{R})}. \quad (19)$$

To propagate with $\tilde{G}_2(\mathbf{R}',\mathbf{R},\tau)$, we need to sample from a normalized probability density and then reweight by the ratio of $\tilde{G}_2(\mathbf{R}',\mathbf{R},\tau)$ to that density. A good choice is the drift-diffusion projector in Eq. (A27), but with the drift velocity given by

$$\mathbf{V}(\mathbf{R}) = \left. \frac{\nabla_{\mathbf{R}'} \tilde{G}_2(\mathbf{R}',\mathbf{R},\tau)}{\tilde{G}_2(\mathbf{R}',\mathbf{R},\tau)} \right|_{\mathbf{R}'=\mathbf{R}}, \quad (20)$$

provided that Ψ_G is nodeless. Note that if $\tilde{G}_2(\mathbf{R}',\mathbf{R},\tau)$ is replaced by the usual drift-diffusion-reweighting form of the importance sampled projector, $\tilde{G}(\mathbf{R}',\mathbf{R},\tau)$, but with the reweighting term evaluated only at $\mathbf{R}$, then $\mathbf{V}(\mathbf{R})$ reduces to the usual $\mathbf{V}(\mathbf{R})$ in Eq. (A26).

Since we want $|\Psi_G| \propto |\Psi_T|$ far from the nodes of Ψ_T, a good nodeless Ψ_G is $\Psi_G = f(d)|\Psi_T|$, with the $f(d)$ in Eq. (A17) and d in Eq. (A15). (Other choices are possible. Refs. 31 and 56 use

$$d = \frac{(\mathrm{Det}(\phi_k(\mathbf{r}_i)))^2}{\prod_i \sum_k \phi_k^2(\mathbf{r}_i)} \quad (21)$$

and

$$d = \frac{1}{\sum_{i,j} |A^{-1}_{ij}|^2} \quad (22)$$

respectively,[57] where ϕ_k are the orbitals in the determinant and A^{-1} is the inverse of the Slater matrix.) Note that this Ψ_G does not cause large weight fluctuations, because its local energy is not being used in a reweighting term. Note also that one can use $\Psi_G = \Psi_T$, but something other than the drift-diffusion projector would need to be used to propose moves in order avoid imposing a FN constraint. If $\Psi_G = \Psi_T$, for the energy estimate, $n = 1$ and $m = 0$ at the nodes of Ψ_T (see the Appendix), so the statistical error of the energy converges to zero as $\sqrt{\ln(N_{MC})/N_{MC}}$, whereas for a nodeless Ψ_G, $n = 0$ and $m = 0$ at the nodes of Ψ_T and the usual $\sqrt{1/N_{MC}}$ convergence is obtained.

A. Cancellations

Since the sign of the contributions to the expectation values is the sign of the product of the walker weights and $\Psi_T(\mathbf{R}')/\Psi_G(\mathbf{R}')$, we will speak about *positive and negative contribution walkers*. The MC run is started with positive contribution walkers only. However, upon evolving walkers with the $\tilde{G}_2(\mathbf{R}',\mathbf{R},\tau)$ of Eq. (19), their contribution can change sign. Hence, it is necessary to devise a mechanism for opposite sign contribution walkers to meet and cancel.

1. Internal cancellations

Note that relative to a 1st-quantized approach, we have internal cancellations in our 2nd-quantized approach because odd and even permutations of electrons in the initial walker contribute with opposite sign to a given permutation in the propagated walker. At large τ, in the absence of time step error, the true projectors (with or without importance sampling[58]) are close to the corresponding fixed-node projectors provided that Ψ_T is a good approximation to Ψ_0, even though at small τ they are very different.[59] This is because $\lim_{\tau\to\infty} G_2(\mathbf{R}',\mathbf{R},\tau) \propto \Psi_0(\mathbf{R}')$. So, using a 2nd-quantized continuous real-space basis and the exponential projector, the sign problem becomes less severe with increasing τ. This is as expected since the internal cancellations within a 2nd-quantized walker are more effective at large τ.

The internal cancellations within a walker ameliorate the sign problem but do not eliminate it (except in the $\tau \to \infty$ limit). So, we need to cancel walkers that are not related by symmetry. When the QMC walk is in a discrete space (e.g., in S-FCIQMC), opposite contribution walkers[60] cancel when they land on the same state. When the walk is in a continuous space (DMC), walkers never land on the same state by accident, but one can alter the walker dynamics to force them to land on the same state, without introducing any bias in the expectation values. There exist exact methods, e.g., those developed by Kalos and coworkers[48–52] to drive the walkers to land on the same state, thereby allowing cancellations.

2. Walker pairing

At each MC step, each negative contribution walker is paired with a positive contribution walker, the latter being

much more numerous. For these methods to be efficient (reasonably small weight fluctuations), it is important that each member of the pair starts off at a distance that is comparable to, or smaller than, the extent of the projector. Hence, it is crucially important that $\tilde{G}_2(\mathbf{R}', \mathbf{R}, \tau)$ have a small time step error, so that a large enough τ can be employed. One needs to identify which pairs (or larger groups) of walkers are close, taking into consideration that the electrons of one walker can be permuted to minimize the distance. It may seem that this entails an $O(N!)$ computational cost, but the cost can be reduced to $O(N^3)$. First, a coarse grouping of walkers can be made by dividing 3D space into boxes and calculating occupation numbers for the boxes. (Unlike the discrete case, the occupation numbers are of course not limited to 0 and 1 any more.) This step takes just $O(N)$ time. Then, each negative contribution walker is paired with the positive contribution walker that is closest to it from among the small group of walkers that have the same occupation numbers (provided there are some) using the Hungarian algorithm[61] for the assignment problem. This algorithm takes only N^3 time to identify the permutation that minimizes the distance between two walkers.

When the paired walkers are sufficiently close, they can be cancelled efficiently by forcing them to move to the same state in a single step, as discussed next. If they are not sufficiently close, then the paired walkers undergo a correlated dynamics that bring them closer over the next several steps,[48–52] as discussed in Section IV A 4.

3. Correlated dynamics for single-step cancellations

A pair of opposite contribution walkers at $\mathbf{R}_1$ and $\mathbf{R}_2$ can be moved to the same state in various ways. We present one, which avoids large weight fluctuations. Pick one of the two walkers, each with probability half. Assume, for the rest of this discussion that the first walker is picked; the other case is completely analogous. Sample a move from $G_{\mathrm{DD}}(\mathbf{R}'_1, \mathbf{R}_1, \tau)$ in Eq. (A27) with the $\mathbf{V}(\mathbf{R})$ in Eq. (20). The probability density for sampling this point is $\rho = \left(G_{\mathrm{DD}}(\mathbf{R}'_1, \mathbf{R}_1, \tau) + G_{\mathrm{DD}}(\mathbf{R}'_1, \mathbf{R}_2, \tau)\right)/2$, since picking either walker can result in a move to $\mathbf{R}'_1$. The weight multiplier for the two walkers is $\tilde{G}_2(\mathbf{R}'_1, \mathbf{R}_1, \tau)/\rho$ and $\tilde{G}_2(\mathbf{R}'_1, \mathbf{R}_2, \tau)/\rho$, respectively. Now that they are at the same point, if their contributions have opposite sign, the portion of the weight equal to the lesser of the two absolute weights can be cancelled. Note that even though we start the move with two opposite contribution walkers, they can end the move with contributions of the same sign. In that case the contributions add, and if the sum is negative we pair this walker with a different walker that has positive contribution, to enable cancellation for the next move.

4. Correlated dynamics for multi-step cancellations

If the starting positions of the two walkers are not close compared to the extent of the projector, the cancellation will not be effective because even if they begin a move with similar absolute weights, they can acquire very different absolute weights during the move. Hence, instead of forcing a pair of opposite-sign walkers to move to the same position in a single step, alter the pair dynamics such that they get closer together on average over several steps and eventually cancel.[49,52] The basic idea is to change the pair dynamics while leaving the individual dynamics unchanged. The first walker in the pair diffuses just as it does in the usual algorithm. The diffusion of the second walker in the pair is correlated to the diffusion of the first walker in the following way. The diffusion is resolved into a component parallel to the line joining the two walkers and a perpendicular component. The perpendicular component for the second walker is the same as for the first walker. The parallel component for the second walker is opposite that of the first walker. In other words, the diffusion of the second walker is the reflection of the diffusion of the first walker in the plane perpendicular to the line joining them in $3N$-dimensional space. So, the distance between the walkers undergoes a 1-dimensional random walk. If the starting distance is R, one can expect that the walkers will meet in $O(R^2/\tau)$ Monte Carlo steps, since the expected diffusion is $O\left(\sqrt{\tau}\right)$ in one step and $O\left(\sqrt{N_{\mathrm{MC}}\tau}\right)$ in N_{MC} steps. Note that the drift step does not alter this analysis because the drift of two walkers that start off reasonably close is strongly correlated anyway. Note also that this paired dynamics does not introduce any bias, as seen from the following argument. Each walker contributes to the expectation value, independently of all other walkers. So, all that is required is that the correlated dynamics of pairs of walkers does not alter the stochastic dynamics of individual walkers. This is in fact the case as seen from the following argument. Consider a large number of identical replicas of the system that are propagated one step using different random numbers for each replica. If one just looked at the dynamics of just one of the paired walkers in each replica, there is no way to tell that one is performing this paired dynamics and not the usual dynamics. Just to make the point more clearly, note that if we were to modify the dynamics so that the second walker in the pair reflected the parallel component of the move only when doing so would make the distance between them shorter, then that would introduce a bias since observing just the second walker we would see that it tends to move in a certain direction (the *a priori* unknown direction of the first walker) in all replicas.

B. Effectiveness of cancellations

As the number of electrons, N, increases, the relative importance of internal cancellations to inter-walker cancellations increases. The reason is that the average distance between two 2nd-quantized walkers increases with increasing N. On the other hand, the effectiveness of internal cancellations depends on the distance between the two closest electrons within a walker and this distance goes down with increasing N. Hence, the use of 2nd-quantized walkers and internal cancellations, which have not been taken advantage of in earlier work, are an important ingredient for the success of the method.

V. APPROXIMATE PMC METHODS BEYOND THE FIXED-NODE APPROXIMATION

Since the exact algorithm is likely to work only for small systems, we now discuss using the projector presented in

Section IV in two approximate methods that have smaller errors than the FN approximation and are applicable to larger systems.

A. Release-node method

In fixed-node calculations, the projection is performed subject to the boundary condition that the projected state vanish at the nodes of Ψ_T. Since $\Psi_T > 0$ and $\Psi_T < 0$ regions map onto each other, the walk can be constrained to $\Psi_T > 0$ regions. In the release-node method,[21,31,32] walkers can cross into $\Psi_T < 0$ regions but are killed if they have been in the $\Psi_T < 0$ region for M consecutive generations. As M is increased, the energy drops from the fixed-node energy to the energy of the fermionic ground state. However, the statistical error increases with increasing M since the bosonic ground state is the dominant state in the absence of a fixed-node constraint. Hence, release-node energies that are significant improvements upon fixed-node energies have been obtained for only a few systems, most notably the homogeneous electron gas.[21,31,32] For molecular systems, the boson-fermion energy gap increases with atomic number as Z^3, so the method is feasible for very low Z systems only.[62]

So far the release-node method has been used with the usual drift-diffusion-reweighting projector and a nodeless guiding function of the form,[31]

$$\Psi_G = |\Psi_T| \left(1 + \epsilon \frac{\prod_i \sum_k \phi_k^2(\mathbf{r}_i)}{(\mathrm{Det}(\phi_k(\mathbf{r}_i)))^2} \right)^{1/2}, \tag{23}$$

where ϕ_k are the orbitals in the determinantal part of Ψ_T. One problem with this is that the local kinetic energy is very negative in the region near the nodes of Ψ_T, so the walkers in that region acquire very large absolute weights, resulting in a large increase in the statistical error. Instead, we use the projector specified in Eqs. (15), (16), (18), and (19) which does not have this problem and has the advantage of having internal cancellations.

B. Stochastic reconfiguration

The idea behind the stochastic reconfiguration method[63,64] is that rather than cancelling walkers that are on the same state, which is hard to arrange for large systems, instead cancel walkers such that the contributions to certain expectation values are unchanged. At each MC generation, there are three sets of weights: (a) w_i, resulting from propagation by the true projector, (b) w_i^f, which are a set of reference weights that are chosen to be non sign-violating (defined below), and (c) w_i^r, the reconfigured weights, which are deduced from the other two sets of weights and are close to the reference weights and therefore mostly non sign-violating. The index i is for the walker number. The original method assumed that importance sampling is used with $\Psi_G = \Psi_T$, but we consider the more general case when $\Psi_G \neq \Psi_T$. In that case, it is useful to define,

$$\tilde{w}_i = w_i \frac{t_i}{g_i}, \qquad \tilde{w}_i^f = w_i^f \frac{t_i}{g_i}, \qquad \tilde{w}_i^r = w_i^r \frac{t_i}{g_i}. \tag{24}$$

A weight w_i is said to be sign-violating if $\tilde{w}_i < 0$.

The reference weights can be chosen to be the fixed-node weights. With this choice, in DMC, the weights, w_i and w_i^f can be computed as follows. First pick which probability density, exact or FN, to sample with equal probability. If the exact one is chosen, sample a point from $G_{DD}(\mathbf{R}', \mathbf{R}, \tau)$ in Eq. (A27) with the $\mathbf{V}(\mathbf{R})$ in Eq. (20). If the FN one is chosen, sample a point from $G_{DD}(\mathbf{R}', \mathbf{R}, \tau)$ in Eq. (A27) with the $\mathbf{V}(\mathbf{R})$ in Eq. (A26). Evaluate each of the probability densities at the sampled point and call these ρ_{exact} and ρ_{FN}. The chosen point has now been sampled with probability density $\rho = (\rho_{\mathrm{exact}} + \rho_{\mathrm{FN}})/2$. The exact weight multiplier is $\tilde{G}_2(\mathbf{R}', \mathbf{R}, \tau)$ in Eqs. (19) and (20) divided by ρ, and the FN weight multiplier is $\tilde{G}(\mathbf{R}', \mathbf{R}, \tau)$ in Eqs. (A25) and (A26) divided by ρ. The new ingredient proposed here is the use of $\tilde{G}_2(\mathbf{R}', \mathbf{R}, \tau)$ in Eqs. (19) and (20). The internal cancellations in $\tilde{G}_2(\mathbf{R}', \mathbf{R}, \tau)$ make the stochastic reconfiguration algorithm more accurate and efficient.

The reconfigured weights, w_i^r, are computed imposing the condition that for this MC generation the overlap of the projected wavefunction and Ψ_T is unchanged by reconfiguration, i.e., $\sum \tilde{w}_i^r = \sum \tilde{w}_i$ and that generation averages of a chosen set of operators are also unchanged. These conditions are imposed by solving a set of linear equations,[63,64] the number of equations being the number of operator constraints. Although the generation average of the operators is unchanged by reconfiguration, a bias is introduced when one propagates the population to the next generation. This bias goes down but the sign problem reappears with increasing number of operators. As usual, there is a trade-off between reducing the systematic bias and the statistical error. Of course, it is necessary to have a walker population that is larger than the number of operator constraints. Reasonable choices for the operators are components of the energy and the 1- and 2-body densities.

The reference weights were chosen to be an extension of the fixed-node weights in Refs. 63 and 64, but it is simpler to choose $w_i^f = w_i$ if w_i is non sign-violating and $w_i^f = 0$ otherwise. If there is little or no cancellation, and the trial wavefunction is good, as is typically the case in real space methods, then the former choice is a good one. On the other hand, when there is considerable cancellation and the trial wavefunction is not very good, as is typically the case in orbital space methods, then the latter choice may be preferable since the w_i are mostly non sign-violating and the former choice results in more reconfiguration than is necessary. In orbital space methods, there is often the complication that the trial wavefunction is zero on most states. Hence, it is not clear which weights are sign-violating. Further, the local energy is $\pm\infty$ for states that are connected to Ψ_T but not in Ψ_T, and it is undefined on states that are not connected to Ψ_T. However, the SR method can still be used, even when the energy is the only quantity that is constrained, with the following simple modifications. Weights, w_i, are deemed to be sign-violating either if $w_i t_i / g_i < 0$ or if $t_i = 0$ and $w_i (\sum_j H_{ij} t_j)/g_i > 0$. Set w_i^f to zero if w_i is sign violating and set $w_i^f = w_i$ otherwise. Note $w_i^f = w_i$ for states not connected to Ψ_T. Further, to avoid numerical problems, for states not connected to Ψ_T, $\sum_j H_{ij} t_j$ is set to a completely negligible constant and the local energy of states that are not in Ψ_T is set to a finite constant. In the S-FCIQMC method, the local energy is the variational energy for all states within Ψ_T. Hence, when only the energy is constrained by the reconfiguration, the ratio, w_i^r / w_i, takes only two values for

non sign-violating weights at each MC step: one for the states within Ψ_T and another for the states outside Ψ_T. Typically, the former is only slightly less than 1. A slight modification of the above results in three values of w_i^r/w_i for non sign-violating weights, one for states in Ψ_T, another for states connected to Ψ_T but not in Ψ_T, and a third for states not connected to Ψ_T. Using SR allows one to use a smaller value for the initiator threshold in S-FCIQMC. However, since SR introduces a bias, it is not *a priori* clear whether the overall bias in reduced or increased by adding SR to the S-FCIQMC algorithm, in those situations where the initiator bias is not negligible. Preliminary studies indicate it is sometimes reduced.

VI. DISCUSSION

In this paper, we have presented a unified description of VMC and various PMC methods, both those that work in a finite discrete Hilbert space and those that work in an infinite continuous Hilbert space. Some of the points made are known but possibly not widely appreciated. The main new contributions are as follows.

(a) A method for performing FN-DMC calculations efficiently using a nodeless Ψ_G ($\Psi_G \neq \Psi_T$), which is helpful for constructing finite-variance estimators for some observables and
(b) a DMC method for doing exact calculations for fermions, which can use either a nodeless Ψ_G or $\Psi_G = \Psi_T$.

At present, the S-FCIQMC method has been much more successful than methods based on DMC for computing almost exact energies of small systems and systems where the sign problem is not severe, e.g., the homogeneous electron gas at small r_s. However, each method has significant advantages and disadvantages relative to the other, so it is not clear whether the ideas presented in this paper will change this situation. Here is a comparison.

1. The S-FCIQMC works with 2nd-quantized walkers. Although current implementations of DMC work with 1st-quantized walkers, which is a significant disadvantage, in this paper we have proposed a way to work with 2nd-quantized walkers without changing the computational scaling.
2. The S-FCIQMC method has the obvious advantage, since it works in a discrete space, that cancellations can occur of their own accord. The DMC method allows one to perform correlated walks that enable cancellations.
3. The wavefunction in the S-FCIQMC method is typically concentrated in a small part of Hilbert space. This is crucial for the success of the method as it greatly enhances the cancellation probabilities. The wavefunction in DMC is much more spread out. This disadvantage is somewhat ameliorated by being able to use a larger time step and by being able to do correlated walks that end in cancellation.
4. The S-FCIQMC method has no time step error. The DMC method has a time step error but can typically use larger time steps than S-FCIQMC while still having a sufficiently small error.
5. The cost per 2-electron move in the S-FCIQMC method scales as $O(1)$ for approximate uniform moves and as $O(N)$ for approximate heat-bath moves (which are nevertheless more efficient). Both 1- and 2-electron moves are possible; most are 2-electron. In addition, there is an $O(N^2)$ cost for calculating the diagonal matrix element for newly occupied determinants. The cost per move in the DMC method scales as $O(N^3)$ for moving all N electrons regardless of whether the accept/reject step is done after 1-electron moves or after moving all electrons.
6. The trial wavefunction Ψ_T in S-FCIQMC is limited to being a sum of determinants. The trial wavefunction Ψ_T in DMC is much more flexible, e.g., it has a Jastrow part and sometimes also backflow terms in the determinants.
7. The S-FCIQMC method has finite-basis errors that are greatly reduced by using the F12 approach. Also, some of the finite-basis errors cancel out when computing energy differences. The DMC method works directly with an infinite basis.
8. Heavy atom systems can be treated with the frozen-core approximation in S-FCIQMC. Efficient calculations of heavy atom systems require the use of a pseudopotential in DMC which typically introduces a larger error than the frozen-core approximation error.
9. The density matrix version of the S-FCIQMC method provides access to a range of observables. The calculation of expectation values of operators that do not commute with the Hamiltonian requires additional computational effort in DMC.

If no approximations are made, both methods suffer from an exponential cost with increasing N. Hence, we have also presented ideas for two approximate DMC methods, applicable to larger systems, that have smaller errors than those of the commonly used fixed-node approximation.

ACKNOWLEDGMENTS

I thank Bryan Clark, Julien Toulouse, Garnet Chan, Shiwei Zhang, Sandro Sorella, David Ceperley, Roland Assaraf, Ali Alavi, George Booth, and Gennady Samorodnitsky for valuable discussions and some of them at the Telluride Science Research Center. This work was supported in part by Grant Nos. NSF CHE-1112097 and DOE-CMCSN DE-SC0006650.

APPENDIX: OPTIMAL IMPORTANCE SAMPLING

We discuss possible choices for the distribution sampled in VMC and DMC. For some observables, the usual choice, Ψ_T^2 in VMC and $\Psi_{FN}\Psi_T$ in DMC, results in large or even infinite variance.

We will be rather cavalier about distinguishing between quantum mechanical expectation values and MC estimates of these expectation values, using at times the same notation for them. However, the intended meaning should be clear from the context.

If we wish to compute an integral

$$I = \langle f \rangle, \tag{A1}$$

using Monte Carlo methods, the statistical error can be reduced by using importance sampling, i.e., by sampling from a

distribution $\tilde{f}$ that mimics the integrand, f, and whose integral is known. It is well known that the optimal distribution to sample from is $\frac{|f|}{\langle|f|\rangle}$, since the sampled distribution must be nonnegative. If f is entirely of one sign, then this optimal sampling distribution gives a zero-variance estimator. Of course in most cases, we do not know $\langle|f|\rangle$. So, in practice we use a function $\tilde{f}$ which approximates the optimal function and whose integral, $\langle\tilde{f}\rangle$ is known. Then

$$I = \left\langle \frac{f}{\tilde{f}} \right\rangle_{\tilde{f}} \langle\tilde{f}\rangle, \tag{A2}$$

where $\langle x\rangle_{\tilde{f}}$ denotes a MC average of x using points sampled from $\frac{\tilde{f}}{\langle\tilde{f}\rangle}$.

Instead, in quantum mechanics, one frequently wishes to compute ratios of expectation values,

$$E = \frac{\langle f\rangle}{\langle g\rangle}. \tag{A3}$$

Then, one possibility is to separately importance sample the numerator and the denominator. The problem is that it is often difficult to find two functions, one of which is close to the absolute value of the numerator and the other to the absolute value of the denominator and whose integrals are known. Further, one would like to avoid the computational expense of doing two separate Monte Carlo runs for the numerator and the denominator.

Instead, one can use the same probability distribution, ρ, to sample the numerator and the denominator. In that case, it is not necessary to know the integral of the function because it cancels out. We get

$$E = \frac{\langle f/\rho\rangle_\rho}{\langle g/\rho\rangle_\rho}. \tag{A4}$$

A common choice for ρ is $\rho = g$ in which case

$$E = \frac{\langle f/g\rangle_g}{\langle 1\rangle_g}. \tag{A5}$$

Although this is a zero-variance estimator for the denominator, it does not minimize the statistical error of the quantity of interest. In fact, the optimal distribution to sample from is[65–68]

$$\rho_{\rm opt} = \left| f - \frac{\langle f\rangle}{\langle g\rangle} g \right|. \tag{A6}$$

One may wonder why this $\rho_{\rm opt}$ reduces to $|f - \langle f\rangle|$ rather than $|f|$ when $g = \mathbf{1}$. The reason is that $|f|$ is the optimal distribution if $\langle|f|\rangle$ is known and $|f - \langle f\rangle|$ is the optimal distribution that does not require knowing $\langle|f|\rangle$. Note that in Eq. (A6), the quantity we want to compute $\frac{\langle f\rangle}{\langle g\rangle}$ appears in $\rho_{\rm opt}$. However, this is not a serious problem, since one usually has a reasonable estimate, $E_{\rm est}$ with an estimated error ϵ. The optimal distribution then is[67]

$$\rho_{\rm opt} = \sqrt{(f - E_{\rm est} g)^2 + 2g^2\epsilon^2}. \tag{A7}$$

Eqs. (A6) and (A7) are obtained assuming the autocorrelation time, $T_{\rm corr}$, due to the sequential correlations in the Markov chain does not depend on the sampled distribution. This is reasonable since ρ and $T_{\rm corr}$ are independent in the sense that a given ρ can be sampled by various algorithms that may have very different values of $T_{\rm corr}$.

One problem with the above $\rho_{\rm opt}$ is that although one can sample from $\rho_{\rm opt}$ using the Metropolis-Hastings algorithm[18,19] when f and g are explicitly known as in the case of VMC, it may be hard to come up with a sufficiently good proposal matrix to have a short autocorrelation time that can be sampled sufficiently quickly. Hence, it may be better to use a sampling distribution that is suboptimal but can be sampled more efficiently. Further, one is typically interested in calculating more than one expectation value in a MC run, and each expectation value has a different optimal sampling distribution, so one is really interested in a good compromise distribution. In PMC, weighted random walks of a population of walkers are needed, and minimizing the weight fluctuations is an important ingredient for an efficient algorithm.

1. VMC

The VMC energy is

$$E = \frac{\langle\Psi_{\rm T}|\hat{H}|\Psi_{\rm T}\rangle}{\langle\Psi_{\rm T}|\Psi_{\rm T}\rangle} = \frac{\langle\Psi_{\rm T}^2 E_{\rm L}\rangle}{\langle\Psi_{\rm T}^2\rangle}. \tag{A8}$$

The distribution that is usually sampled is $\Psi_{\rm T}^2$ and the expression for the energy is

$$E = \frac{\langle E_{\rm L}\rangle_{\Psi_{\rm T}^2}}{\langle 1\rangle_{\Psi_{\rm T}^2}} \approx \frac{\sum_{i=1}^{N_{\rm MC}} E_{\rm L}(\mathbf{R}_i)}{N_{\rm MC}}. \tag{A9}$$

On the other hand, the optimal distribution, $\rho_{\rm opt}$, from Eq. (A6) is

$$\rho_{\rm opt}(\mathbf{R}) \equiv \Psi_{\rm G}^2(\mathbf{R}) = \Psi_{\rm T}^2(\mathbf{R})\sqrt{(E_{\rm L}(\mathbf{R}) - E_{\rm est})^2 + 2\epsilon^2}, \tag{A10}$$

and the energy can be computed as

$$E \approx \frac{\sum_{i=1}^{N_{\rm MC}} \frac{E_{\rm L}(\mathbf{R}_i)}{\sqrt{(E_{\rm L}(\mathbf{R}_i) - E_{\rm est})^2 + 2\epsilon^2}}}{\sum_{i=1}^{N_{\rm MC}} \frac{1}{\sqrt{(E_{\rm L}(\mathbf{R}_i) - E_{\rm est})^2 + 2\epsilon^2}}}. \tag{A11}$$

As an aside, we note that this estimate has a bias that disappears in the $N_{\rm MC} \to \infty$ limit, and the bias can be reduced by computing the covariance of the summands in the numerator and the denominator. A simpler method for doing the same is described in the Appendix of Ref. 69. Since $\rho_{\rm opt}$ in Eq. (A10) is a known function, it can be sampled using the Metropolis-Hastings algorithm.[18,19] The usual distribution sampled in VMC is $\Psi_{\rm T}^2$ and a good proposal matrix is obtained using $\nabla\Psi_{\rm T}$. Since $\nabla^2\Psi_{\rm T}$ is needed for computing the local energy for the VMC energy estimate, it requires minimal extra computational effort to compute also $\nabla\Psi_{\rm T}$. On the other hand, constructing a good proposal matrix for the optimal sampling distribution requires computing $\nabla E_{\rm L}$, which requires additional computational effort. Hence, it is worth employing simpler sampling distributions that are functions of $\Psi_{\rm T}$ only. This, plus the consideration that other expectation values than the energy may be of interest, is the reason that the usual distribution sampled in VMC is $\Psi_{\rm T}^2$. However, since $E_{\rm L}(\mathbf{R}) \propto 1/\Psi_{\rm T}(\mathbf{R})$ near nodes, we see from Eq. (A10) that sampling a function that goes as $|\Psi_{\rm T}|$ near the nodes is better than the usual choice, $|\Psi_{\rm T}|^2$.

If the sampled probability distribution goes as Ψ_T^n near the nodes of Ψ_T and the integrand of the expectation value of interest goes as Ψ_T^m near the nodes of Ψ_T, then the contribution to the variance from the region up to a distance ϵ from the node is

$$\int_0^\epsilon dx x^n (x^{m-n})^2 \sim \begin{cases} \epsilon^{2m-n+1} & \sim N_{MC}^{n-2m-1}, \quad \text{if } n < 2m+1, \\ \ln(\epsilon) - \ln(0) & \sim \ln(N_{MC}), \quad \text{if } n = 2m+1. \end{cases} \tag{A12}$$

From this, we see that the region near the node makes no contribution to the variance if $n < 2m+1$, but it makes a contribution such that the error of the MC average converges as $\sqrt{\ln(N_{MC})/N_{MC}}$ rather than $1/\sqrt{N_{MC}}$ if $n = 2m+1$.

Hence, if $m = 0$, it is desirable to sample from a ρ that is finite at the nodes of Ψ_T. So, consider ρ of the form,

$$\rho(\mathbf{R}) = \begin{cases} f(d)|\Psi_T(\mathbf{R})|, & d(\mathbf{R}) < \epsilon, \\ |\Psi_T(\mathbf{R})|, & d(\mathbf{R}) \geq \epsilon \end{cases} \tag{A13}$$

and

$$\rho(\mathbf{R}) = \begin{cases} (f(d)\Psi_T(\mathbf{R}))^2, & d(\mathbf{R}) < \epsilon, \\ \Psi_T^2(\mathbf{R}), & d(\mathbf{R}) \geq \epsilon, \end{cases} \tag{A14}$$

where

$$\mathbf{d}(\mathbf{R}) = \frac{-\Psi_T(\mathbf{R})\nabla\Psi_T(\mathbf{R})}{|\nabla\Psi_T(\mathbf{R})|^2} \tag{A15}$$

is the vector to the estimated nearest point on the nearest nodal surface and $d = |\mathbf{d}|$. If we impose the conditions that ρ be continuous and have continuous first derivative at $d = \epsilon$ (though these conditions are not necessary), $f(d)$ must satisfy

$$\begin{aligned} f(d) &= 1, && \text{when } d = \epsilon, \\ \frac{df(d)}{dd} &= 0, && \text{when } d = \epsilon, \\ d \times f(d) &= \text{const} \times \epsilon, && \text{when } d = 0. \end{aligned} \tag{A16}$$

A reasonable choice for $f(d)$ is

$$f(d) = \frac{1}{2}\left(\frac{\epsilon}{d} + \frac{d}{\epsilon}\right). \tag{A17}$$

These ideas were tested on a toy example (particle in a box). Two ratios of expectation values, which are of interest in VMC calculations, were studied in Table II. The first is the variational energy, $E = \langle\Psi_T|H|\Psi_T\rangle/\langle\Psi_T|\Psi_T\rangle$ and the second is its derivative, $E_i = \langle\Psi_{T,i}|(H-E)|\Psi_T\rangle/\langle\Psi_T|\Psi_T\rangle$, with respect to a variational parameter, p_i. $\Psi_{T,i}$ is the derivative of Ψ_T with respect to p_i. For approximate Ψ_T, E_L typically diverges as the inverse of the distance to the nodes of Ψ_T. The parameter was chosen (as detailed in the caption of Table II) to be such that the nodes of Ψ_T depend on the value of the parameter. In that case, Ψ_i/Ψ_T also diverges as the inverse of the distance to the nodes of Ψ_T. So, m in Eq. (A12) is 1 for E and it is 0 for E_i.

TABLE II. Values of $\sqrt{N_{MC}}\sigma_E$ and $\sqrt{N_{MC}}\sigma_{E_i}$, using various choices of the sampling distribution ρ for a particle in a box and with an approximate $\Psi_T = \sin(\pi(x + (x^2 - bx^3))/2)$, with $b = 1$ and $\epsilon = 0.1$. When $\rho = \Psi_T^2$ or $\rho = |\Psi_T|$, $\sqrt{N_{MC}}\sigma_{E_i}$ is infinite for an infinite sample. For a finite sample, the estimated value of $\sqrt{N_{MC}}\sigma_{E_i}$ increases with sample size, as shown. A logarithmic divergence is acceptable since σ_{E_i} converges as $\sqrt{\ln(N_{MC})/N_{MC}}$.

Sampled Fn. ρ	$\sqrt{N_{MC}}\sigma_E$	$\sqrt{N_{MC}}\sigma_{E_i}$
1	1.832	4.252
$\sqrt{\lvert\Psi_T\rvert}$	1.740	6.645
$\lvert\Psi_T\rvert$	1.817	$\infty \sim \sqrt{\ln(N_{MC})}$
$\lvert\Psi_T\rvert^2$	2.641	$\infty \sim \sqrt{N_{MC}}$
$1 + \lvert\Psi_T\rvert^2$	1.774	4.701
Eq. (A13)	1.815	7.860
Eq. (A14)	2.401	20.049
Optimal Eq. (A6)	1.530	3.341

In Table II we give, for various choices of ρ, values of $\sqrt{N_{MC}}\sigma$, where σ is the estimated root mean square error of the mean. For a finite-variance estimator, $\sqrt{N_{MC}}\sigma$ tends to a finite value with increasing N_{MC}, whereas for an infinite-variance estimator $\sqrt{N_{MC}}\sigma \to \infty$ as shown in the table. The value of ϵ in Eqs. (A13) and (A14) can be tuned to minimize the variance, but the results in Table II were obtained simply by setting $\epsilon = 0.1$. The MC estimate of E_i has finite variance for $\rho = 1$ or $\rho = 1 + \Psi_T^2$, but these choices of ρ are feasible only when the integration domain is finite. The optimal ρ of Eq. (A6) of course gives the smallest value of $\sqrt{N_{MC}}\sigma$. For this example, of the choices of ρ that were studied, the usual choice in VMC calculations, $\rho = \Psi_T^2$, gives the largest error. However, in typical VMC calculations of fermionic many-body systems, the values of Ψ_T at the sampled points have a range of many orders of magnitude and the fluctuations of E_L do not correlate strongly with the value of Ψ_T except very close to the nodes of Ψ_T, so $\rho = \Psi_T^2$ is a reasonable choice for computing the energy. A better choice for computing the energy would be $\rho \sim |\Psi_T|$ near the nodes and $\rho \sim \Psi_T^2$ away from the nodes and a good choice for the energy derivatives would have a finite ρ near the nodes and $\rho \sim \Psi_T^2$ away from the nodes, such as the ρ in Eq. (A14).

2. Fixed-node DMC

For computing the DMC energy, the optimal sampling distribution of Eq. (A6) becomes

$$\begin{aligned} \rho_{opt}(\mathbf{R}) &\equiv |\Psi_{FN}(\mathbf{R})\Psi_G(\mathbf{R})| \\ &= |\Psi_{FN}(\mathbf{R})\Psi_T(\mathbf{R})|\sqrt{(E_L(\mathbf{R}) - E_{est})^2 + 2\epsilon^2}. \end{aligned} \tag{A18}$$

It is feasible to sample this distribution by similarity transforming the projector with a diagonal matrix with diagonal components $\Psi_T\sqrt{(E_L - E_{est})^2 + 2\epsilon^2}$. However, as in VMC, the computational effort of constructing a good proposal matrix is sufficiently large that it is useful to consider simpler alternatives. The usual choice, $\rho(\mathbf{R}) = |\Psi_{FN}(\mathbf{R})\Psi_T(\mathbf{R})|$ (i.e., $\Psi_G(\mathbf{R}) = \Psi_T(\mathbf{R})$), is an adequate choice for some observables and efficient algorithms for sampling it are well known.[22,23] However, since E_L diverges at the nodes of Ψ_T, a nodeless Ψ_G that approximates $|\Psi_T|$ far from the nodes of Ψ_T is preferable to $\Psi_G = \Psi_T$ for calculating the energy. For the parameter derivatives

of the energy, choosing $\Psi_G = \Psi_T$ results in infinite variance estimators so it is even more important to use a nodeless Ψ_G.

Since there does not exist an efficient algorithm in the literature for sampling $\Psi_G\Psi_{FN}$ when $\Psi_G \neq \Psi_T$ we present one here. A special case is $\Psi_G = \mathbf{1}$. First, note that the usual projector,

$$G(\mathbf{R}',\mathbf{R},\tau) = \frac{1}{(2\pi\tau)^{\frac{3N}{2}}} e^{-\frac{(\mathbf{R}'-\mathbf{R})^2}{2\tau}+\tau\left(E_T-\frac{\mathcal{V}(\mathbf{R}')+\mathcal{V}(\mathbf{R})}{2}\right)}, \tag{A19}$$

has free boundary conditions rather than fixed-node boundary conditions and therefore cannot be used in fixed-node calculations without modifications. In addition, as is well known, it is not practical to use this form of $G(\mathbf{R}',\mathbf{R},\tau)$ since the potential energy $\mathcal{V}$ can diverge to $\pm\infty$.

Instead, $\Psi_G(\mathbf{R})\Psi_{FN}(\mathbf{R})$ can be sampled efficiently as follows. Note that $f(\mathbf{R}) = \Psi_G(\mathbf{R})\Psi_T(\mathbf{R})$ satisfies

$$\frac{-1}{2}\nabla^2 f(\mathbf{R}) + \nabla\cdot(\mathbf{V}(\mathbf{R})f(\mathbf{R})) = 0, \tag{A20}$$

where

$$\mathbf{V}(\mathbf{R}) = \frac{1}{2}\left(\frac{\nabla\Psi_G(\mathbf{R})}{\Psi_G(\mathbf{R})} + \frac{\nabla\Psi_T(\mathbf{R})}{\Psi_T(\mathbf{R})}\right). \tag{A21}$$

$\Psi_{FN}(\mathbf{R})$ is the ground state solution of the time independent Schrödinger equation with the boundary condition that it has the same nodes as Ψ_T. Multiplying it by $\Psi_G(\mathbf{R})$ we see that $f(\mathbf{R}) = \Psi_G(\mathbf{R})\Psi_{FN}(\mathbf{R})$ is a solution of

$$\frac{-1}{2}\nabla^2 f(\mathbf{R}) + \nabla\cdot(\mathbf{V}(\mathbf{R})f(\mathbf{R})) - S(\mathbf{R})f(\mathbf{R}) = 0, \tag{A22}$$

in the limit $\Psi_T(\mathbf{R}) = \Psi_{FN}(\mathbf{R})$, where

$$S(\mathbf{R}) = E_T - E_L(\mathbf{R}), \tag{A23}$$

which is defined in terms of the local energy

$$E_L(\mathbf{R}) = \frac{\mathcal{H}\Psi_T(\mathbf{R})}{\Psi_T(\mathbf{R})} = -\frac{\nabla^2\Psi_T(\mathbf{R})}{2\Psi_T(\mathbf{R})} + \mathcal{V}(\mathbf{R}). \tag{A24}$$

Hence, it is plausible that an approximate projector is

$$\tilde{G}(\mathbf{R}',\mathbf{R},\tau) \approx \frac{1}{(2\pi\tau)^{\frac{3N}{2}}} e^{\frac{-\left(\mathbf{R}'-(\mathbf{R}+\bar{\mathbf{V}}(\mathbf{R}))\tau\right)^2}{2\tau}+\tau\left(\frac{\bar{S}(\mathbf{R}')+\bar{S}(\mathbf{R})}{2}\right)}, \tag{A25}$$

where $\bar{\mathbf{V}}(\mathbf{R})$ and $\bar{S}(\mathbf{R})$ are estimates of the average $\mathbf{V}$ and S over the time step[23] with initial position $\mathbf{R}$. This is exactly the same as the usual FN-DMC projector except that $\mathbf{V}(\mathbf{R})$ is given by Eq. (A21) rather than

$$\mathbf{V}(\mathbf{R}) = \frac{\nabla\Psi_T(\mathbf{R})}{\Psi_T(\mathbf{R})}. \tag{A26}$$

Hence as usual, walkers are propagated by first sampling from the drift-diffusion part of the projector

$$G_{DD}(\mathbf{R}',\mathbf{R},\tau) = \frac{1}{(2\pi\tau)^{\frac{3N}{2}}} e^{\frac{-\left(\mathbf{R}'-(\mathbf{R}+\bar{\mathbf{V}}(\mathbf{R}))\tau\right)^2}{2\tau}}, \tag{A27}$$

and then reweighted with $\exp\left[\tau\left(\frac{\bar{S}(\mathbf{R}')+\bar{S}(\mathbf{R})}{2}\right)\right]$. As usual, a Metropolis-Hastings accept/reject step can be inserted, but with the modified acceptance probability,

$$A(\mathbf{R}',\mathbf{R},\tau) = \min\left\{1, \frac{|\Psi_G(\mathbf{R}')\Psi_T(\mathbf{R}')|G_{DD}(\mathbf{R},\mathbf{R}',\tau)}{|\Psi_G(\mathbf{R})\Psi_T(\mathbf{R})|G_{DD}(\mathbf{R}',\mathbf{R},\tau)}\right\}, \tag{A28}$$

between the drift-diffusion step and the reweighting step to reduce the time step error,[22,23] in which case an effective time step, τ_{eff}, is used in the reweighting to take into account that some moves are rejected. Also as usual, the accept-reject step can be done either after each one-electron move or after all electrons have been moved, the former usually being more efficient.

There are several things to note.

1. Ψ_G enters only in $\mathbf{V}(\mathbf{R})$ and not in $\bar{S}$. So, although we can use the same Ψ_G as is used in release-node calculations,[31] we do not have the problem of large weight fluctuations near the nodes of Ψ_T.
2. Just as in the usual FN-DMC algorithm, since the velocity diverges at the nodes of Ψ_T, there is no flux of walkers through the nodes *per unit time* in the $\tau \to 0$ limit.
3. The method reduces to the usual FN-DMC if $\Psi_G = \Psi_T$.
4. Unlike the usual FN-DMC method, the distribution $\Psi_G\Psi_0$ is obtained only in the $\Psi_T = \Psi_0$ limit rather than in the limit that the nodes of Ψ_T are the same as those of Ψ_0. In this respect, the method is similar to the discrete-space FN method.[9]
5. Finally, note that we have provided a plausible argument that rests on Eq. (A22) rather than a proof which would require that $f(\mathbf{R},t) = \Psi_G(\mathbf{R})\Psi(\mathbf{R},t)$ satisfy
$$\frac{-1}{2}\nabla^2 f(\mathbf{R},t) + \nabla\cdot(\mathbf{V}(\mathbf{R})f(\mathbf{R},t)) - S(\mathbf{R})f(\mathbf{R},t) = -\frac{\partial f(\mathbf{R},t)}{\partial t}. \tag{A29}$$
So, $\Psi_G(\mathbf{R})\Psi_{FN}(\mathbf{R})$ is a solution of Eq. (A29), but we have not proven that it is the dominant eigenstate of the projector in Eq. (A25), though it seems likely that it is. We have however successfully tested the method on a toy problem, a particle in a box.

Another possibility for sampling $\Psi_G(\mathbf{R})\Psi_{FN}(\mathbf{R})$ is to sample points from $G_{DD}(\mathbf{R}',\mathbf{R},\tau)$ of Eq. (A27) and reweight with the ratio $\tilde{G}_{PP,mir}(\mathbf{R}',\mathbf{R},\tau)/G_{DD}(\mathbf{R}',\mathbf{R},\tau)$, where

$$\tilde{G}_{PP,mir}(\mathbf{R}',\mathbf{R},\tau) = \begin{cases} \tilde{G}_{PP}(\mathbf{R}',\mathbf{R},\tau) - \tilde{G}_{PP}(\mathbf{R}',\mathbf{R}+2\mathbf{d},\tau), & \text{if } > 0, \\ 0, & \text{otherwise,} \end{cases} \tag{A30}$$

and $\tilde{G}_{PP}(\mathbf{R}',\mathbf{R},\tau)$ is the pair-product projector used in path-integral Monte Carlo calculations,[55] importance sampled with Ψ_G. $\tilde{G}_{PP,mir}(\mathbf{R}',\mathbf{R},\tau)$ has the required property that $\tilde{G}_{PP,mir}(\mathbf{R}+\mathbf{d},\mathbf{R},\tau) = 0$ to be an approximate fixed-node projector.

3. S-FCIQMC

The analysis of what constitutes good importance sampling is more difficult in S-FCIQMC for at least three reasons. Using the notation of Sec. II, the optimal sampling distribution is

$$\rho_i^{\text{opt}} \equiv |e_i g_i^{\text{opt}}| = |e_i t_i| \sqrt{(E_{\text{L},i} - E)^2 + 2\epsilon^2} = |e_i| \sqrt{\left(\sum_j H_{ij} t_j - E t_i\right)^2 + 2\epsilon^2 t_i^2}. \tag{A31}$$

The first issue is that this formula says that states that are not connected to Ψ_{T} need not be sampled at all. This ignores the fact that states that are not connected to Ψ_{T} change the distribution on states that are connected to Ψ_{T} and therefore must be sampled in order to get the correct expectation value. One could get around this by sampling these states with some small nonzero probability, δ,

$$g_i = \begin{cases} |t_i| \sqrt{(E_{\text{L},i} - E)^2 + 2\epsilon^2}, & \text{if } i \text{ is connected to } \Psi_{\text{T}}, \\ \delta, & \text{otherwise.} \end{cases} \tag{A32}$$

The second issue is that even for a given choice of the sampling distribution, the efficiency depends on the fluctuations of the walker weights. To minimize the weight fluctuations (for a given time step) it is desirable to have a fast algorithm to propose moves with probabilities that are proportional to the projector matrix elements. Recently, two algorithms have been devised that achieve a good approximation to this in the absence of importance sampling, one of which employs the Cauchy-Schwartz inequality applied to two-body integrals,[44] and another that does not.[45] At present, no algorithm exists for sampling the importance sampling projector, $\tilde{P}_{ij}$, in Eq. (7) sufficiently efficiently.

The third issue is that the cancellation of opposite-sign walkers is an essential part of the algorithm, and this is more effective if importance sampling is used since the walkers are then concentrated on a smaller number of states. This consideration is absent in the derivation of ρ^{opt}. This is the likely reason that importance sampling was found to be helpful in Ref. 70.

[1] M. H. Kalos and P. A. Whitlock, *Monte Carlo Methods* (Wiley-Interscience, 1986), Vol. 1.
[2] B. L. Hammond, W. A. Lester, Jr., and P. J. Reynolds, *Monte Carlo Methods in Ab Initio Quantum Chemistry* (World Scientific, Singapore, 1994).
[3] D. M. Ceperley and L. Mitas, *Advances in Chemical Physics* (John Wiley & Sons, 1996), Vol. 93, pp. 1–38.
[4] M. P. Nightingale and C. J. Umrigar, in *Monte Carlo Methods in Chemistry*, Advances in Chemical Physics Vol. 105, edited by D. M. Ferguson, J. I. Siepmann, and D. G. Truhlar (Wiley, NY, 1998), Chap. 4.
[5] *Quantum Monte Carlo Methods in Physics and Chemistry*, NATO ASI Series C Vol. 525, edited by M. P. Nightingale and C. J. Umrigar (Kluwer, Dordrecht, 1999).
[6] W. M. C. Foulkes, L. Mitas, R. J. Needs, and G. Rajagopal, Rev. Mod. Phys. **73**, 33 (2001).
[7] J. Kolorenč and L. Mitas, Rep. Prog. Phys. **74**, 026502 (2011).
[8] J. B. Anderson, J. Chem. Phys. **65**, 4121 (1976).
[9] D. ten Haaf, H. van Bemmel, J. van Leeuwen, W. van Saarloos, and D. Ceperley, Phys. Rev. B **51**, 13039 (1995).
[10] M. Jones, G. Ortiz, and D. Ceperley, Phys. Rev. E **55**, 6202 (1997).
[11] M. P. Nightingale and V. Melik-Alaverdian, Phys. Rev. Lett. **87**, 043041 (2001).
[12] C. J. Umrigar and C. Filippi, Phys. Rev. Lett. **94**, 150201 (2005).
[13] J. Toulouse and C. J. Umrigar, J. Chem. Phys. **126**, 084102 (2007).
[14] C. J. Umrigar, J. Toulouse, C. Filippi, S. Sorella, and R. G. Hennig, Phys. Rev. Lett. **98**, 110201 (2007).
[15] S. Sorella, M. Casula, and D. Rocca, J. Chem. Phys. **127**, 014105 (2007).
[16] J. Toulouse and C. J. Umrigar, J. Chem. Phys. **128**, 174101 (2008).
[17] E. Neuscamman, C. J. Umrigar, and G. K.-L. Chan, Phys. Rev. B **85**, 045103 (2012).
[18] N. Metropolis, A. W. Rosenbluth, M. N. Rosenbluth, A. H. Teller, and E. Teller, J. Chem. Phys. **21**, 1087 (1953).
[19] W. K. Hastings, Biometrika **57**, 97 (1970).
[20] R. C. Grimm and R. G. Storer, J. Comput. Phys. **7**, 134 (1971).
[21] D. M. Ceperley and B. J. Alder, Phys. Rev. Lett. **45**, 566 (1980).
[22] P. J. Reynolds, D. M. Ceperley, B. J. Alder, and W. A. Lester, J. Chem. Phys. **77**, 5593 (1982).
[23] C. J. Umrigar, M. P. Nightingale, and K. J. Runge, J. Chem. Phys. **99**, 2865 (1993).
[24] G. H. Booth, A. J. W. Thom, and A. Alavi, J. Chem. Phys. **131**, 054106 (2009).
[25] D. Cleland, G. H. Booth, and A. Alavi, J. Chem. Phys. **132**, 041103 (2010).
[26] F. R. Petruzielo, A. A. Holmes, H. J. Changlani, M. P. Nightingale, and C. J. Umrigar, Phys. Rev. Lett. **109**, 230201 (2012).
[27] M. H. Kalos, D. Levesque, and L. Verlet, Phys. Rev. A **9**, 2178 (1974).
[28] D. M. Ceperley and M. H. Kalos, in *Monte Carlo Methods in Statistical Physics*, edited by K. Binder (Springer, Berlin, 1979), pp. 145–194.
[29] M. Casula, C. Filippi, and S. Sorella, Phys. Rev. Lett. **95**, 100201 (2005).
[30] S. Zhang and H. Krakauer, Phys. Rev. Lett. **90**, 136401 (2003).
[31] D. M. Ceperley and B. J. Alder, J. Chem. Phys. **81**, 5833 (1984).
[32] Y. Kwon, D. Ceperley, and R. Martin, Phys. Rev. B **48**, 12037 (1993).
[33] M. Calandra Buonaura and S. Sorella, Phys. Rev. B **57**, 11446 (1998).
[34] R. Assaraf, M. Caffarel, and A. Khelif, Phys. Rev. E **61**, 4566 (2000).
[35] M. H. Kolodrubetz, J. S. Spencer, B. K. Clark, and W. M. C. Foulkes, J. Chem. Phys. **138**, 024110 (2013).
[36] G. H. Booth, S. D. Smart, and A. Alavi, Mol. Phys. **112**, 1855 (2014).
[37] J. J. Shepherd, A. Grueneis, G. H. Booth, G. Kresse, and A. Alavi, Phys. Rev. B **86**, 035111 (2012).
[38] G. H. Booth, A. Grueneis, G. Kresse, and A. Alavi, Nature **493**, 365 (2013).
[39] S. Ten-no, J. Chem. Phys. **138**, 164126 (2013).
[40] C. Overy, G. H. Booth, N. S. Blunt, J. J. Shepherd, D. Cleland, and A. Alavi, J. Chem. Phys. **141**, 244117 (2014).
[41] J. S. Spencer, N. S. Blunt, and W. M. C. Foulkes, J. Chem. Phys. **136**, 054110 (2012).
[42] H. Shi and S. Zhang, Phys. Rev. B **88**, 125132 (2013).
[43] W. Purwanto, S. Zhang, and H. Krakauer, J. Chem. Phys. **142**, 064302 (2015).
[44] S. D. Smart, G. H. Booth, and A. Alavi (unpublished results).
[45] A. A. Holmes and C. J. Umrigar, "Efficient heat-bath sampling in Fock space" (unpublished).
[46] D. Arnow, M. Kalos, M. Lee, and K. Schmidt, J. Chem. Phys. **77**, 5562 (1982).
[47] S. Zhang and M. H. Kalos, Phys. Rev. Lett. **67**, 3074 (1991).
[48] Z. Liu, S. Zhang, and M. Kalos, Phys. Rev. E **50**, 3220 (1994).
[49] M. H. Kalos, Phys. Rev. E **53**, 5420 (1996).
[50] F. Pederiva and M. Kalos, Comput. Phys. Commun. **121–122**, 440 (1999).
[51] M. Kalos and F. Pederiva, Physica A **279**, 236 (2000).
[52] M. Kalos and F. Pederiva, Phys. Rev. Lett. **85**, 3547 (2000).
[53] J. B. Anderson, in *Understanding Chemical Reactivity*, edited by S. R. Langhoff (Kluwer, Dordrecht, The Netherlands, 1995).
[54] Y.-S. M. Wu, A. Kuppermann, and J. B. Anderson, Phys. Chem. Chem. Phys. **1**, 929 (1999).
[55] D. M. Ceperley, Rev. Mod. Phys. **67**, 279 (1995).
[56] C. Attaccalite and S. Sorella, Phys. Rev. Lett. **100**, 114501 (2008).

[57] These are proportional to the distance to the node as one approaches the node. The former has the advantage that the gradient and Laplacian can be computed easily. These are required in the drift-diffusion-reweighting form of the projector but not in the projector we use, though having the gradient is helpful for sampling our projector. However, it has the disadvantage that for large systems a small eigenvalue of the Slater matrix can be masked by several large eigenvalues.
[58] Note that unlike the usual FN method, which uses $\Psi_{\text{G}} = \Psi_{\text{T}}$, we consider the more general FN method discussed in the Appendix, wherein Ψ_{G} need not be Ψ_{T} and the projected state has the nodes of Ψ_{T}.
[59] It is easy to see that for small τ, the true projector and the fixed-node projector are very different. For example, for the 1^3S state of the helium atom, the true projector has a nodal surface $(\mathbf{r}_1' - \mathbf{r}_1)^2 + (\mathbf{r}_2' - \mathbf{r}_2)^2$

$= (\mathbf{r}'_1 - \mathbf{r}_2)^2 + (\mathbf{r}'_2 - \mathbf{r}_1)^2$, i.e., $(\mathbf{r}'_1 - \mathbf{r}'_2) \cdot (\mathbf{r}_1 - \mathbf{r}_2) = 0$, whereas the fixed-node projector has a nodal surface $r'_1 = r'_2$.

[60]In S-FCIQMC, "opposite contribution" and "opposite sign" are synonymous because the electrons on a given state are always ordered the same way. In the present algorithm, this cannot be done because we employ whichever permutation minimizes the distance between walkers.

[61]See http://www.en.wikipedia.org/w/index.php?title=Hungarian_algorithm&oldid=655104115 for Hungarian algorithm.

[62]N. M. Tubman, J. L. DuBois, R. Q. Hood, and B. J. Alder, J. Chem. Phys. **135**, 184109 (2011).

[63]S. Sorella, Phys. Rev. Lett. **80**, 4558 (1998).

[64]S. Sorella and L. Capriotti, Phys. Rev. B **61**, 2599 (2000).

[65]Eq. (29) of Ref. 71 reduces to this expression for $m = 1$.

[66]D. M. Ceperley, M. Dewing, and C. Pierleoni, in *Bridging Time Scales: Molecular Simulations for the Next Decade*, edited by M. Mareschal, P. Nielaba, and G. Ciccotti (Springer-Verlag, 2002), pp. 473–500.

[67]J. R. Trail and R. Maezono, J. Chem. Phys. **133**, 174120 (2010).

[68]R. Assaraf, private communication (2014).

[69]J. Toulouse, R. Assaraf, and C. J. Umrigar, in *Advances in Quantum Chemistry*, edited by P. Hoggan and T. Özdoğan (Elsevier, 2015), Vol. 73.

[70]M. H. Kolodrubetz and B. K. Clark, Phys. Rev. B **86**, 075109 (2012).

[71]D. M. Ceperley and B. Bernu, J. Chem. Phys. **89**, 6316 (1988).